Amide proton exchange of a dynamic loop in cell extracts

Austin E. Smith,[1] Mohona Sarkar,[1] Gregory B. Young,[2] and Gary J. Pielak[1,2,3]*

[1]Department of Chemistry, University of North Carolina, Chapel Hill, North Carolina 27599
[2]Department of Biochemistry and Biophysics, University of North Carolina, Chapel Hill, North Carolina 27599
[3]Lineberger Comprehensive Cancer Center, University of North Carolina, Chapel Hill, North Carolina 27599

Received 3 May 2013; Revised 15 July 2013; Accepted 16 July 2013
DOI: 10.1002/pro.2318
Published online 31 July 2013 proteinscience.org

Gary Pielak was an Invited Speaker at the 2013 Protein Society Annual Symposium.

Abstract: Intrinsic rates of exchange are essential parameters for obtaining protein stabilities from amide ^{1}H exchange data. To understand the influence of the intracellular environment on stability, one must know the effect of the cytoplasm on these rates. We probed exchange rates in buffer and in *Escherichia coli* lysates for the dynamic loop in the small globular protein chymotrypsin inhibitor 2 using a modified form of the nuclear magnetic resonance experiment, SOLEXSY. No significant changes were observed, even in 100 g dry weight L^{-1} lysate. Our results suggest that intrinsic rates from studies conducted in buffers are applicable to studies conducted under cellular conditions.

Keywords: amide ^{1}H exchange; macromolecular crowding; NMR; SOLEXSY; solvent exchange

Introduction

The cytoplasm of *Escherichia coli* is a milieu of macromolecules whose total concentration can exceed 300 gL^{-1}.[1,2] This crowded environment is expected to affect biophysical properties, such as protein stability.[3] Quantifying these changes is key to understanding protein chemistry in cells.[4]

^{1}H/^{2}H exchange has been used to assess protein stability since Linderstrøm-Lang and coworkers laid the theoretical framework in the 1950s.[5–7] Native globular proteins exist in equilibrium with a large ensemble of less structured states.[8] When a protein in H_2O is transferred to ^2H_2O, solvent-exposed amide protons in the native state can, in most cases,[9] exchange freely with deuterons. Hydrogen-bonded and other protected protons, however, exchange only upon exposure to solvent during a transient opening [Eq. (1)],

$$\mathrm{N^1H\,(closed)} \underset{}{\overset{K_{op}}{\rightleftharpoons}} \mathrm{N^1H\,(open)} \xrightarrow{k_{int}} \mathrm{N^2H\,(open)} \qquad (1)$$

where $K_{op} = k_{op}/k_{cl}$ is the opening equilibrium constant, k_{op} and k_{cl} are the opening and closing rate constants, respectively, and k_{int} is the intrinsic rate of amide ^{1}H exchange in an unstructured peptide. When intrinsic exchange is rate limiting ($k_{cl} > k_{int}$), the observed exchange rate of a protonated amide (k_{obs}) can be used to determine the modified standard free energy of opening (i.e., the stability), because $k_{obs} = K_{op}k_{int}$ [Eq. (2)].[7,10,11]

$$\Delta G^{\circ\prime}_{op} = -RT\ln K_{op} = -RT\ln\frac{k_{obs}}{k_{int}} \qquad (2)$$

This approach is valid for protons that are exposed on global unfolding, so called "globally exchanging residues," because maximum values of $\Delta G^{\circ\prime}_{op}$ often equal the free energy of denaturation measured by using independent techniques.[7,12,13]

Abbreviations: CI2, chymotrypsin inhibitor 2; CLEANEX-PM, phase-modulated CLEAN chemical exchange; NMR, nuclear magnetic resonance; SASA, solvent accessible surface area; SOLEXSY, solvent exchange spectroscopy.

Additional Supporting Information may be found in the online version of this article.

Grant sponsor: National Science Foundation; Grant number: MCB-1051819.

*Correspondence to: Gary J. Pielak, Department of Chemistry, University of North Carolina, Chapel Hill, NC 27599.
E-mail: gary_pielak@unc.edu

To validate the $^{1}H/^{2}H$ exchange results, one must know if k_{int} changes under crowded conditions. k_{int} values in buffer can be calculated as a function of primary structure, pH, and temperature[14–16] using the online resource, SPHERE.[17] These values have also been used to measure protein stability in solutions crowded by synthetic polymers and proteins, because as described below, these crowding agents do not affect k_{int}.[18–21] Saturation transfer NMR was used to show that the k_{int} of poly-DL-alanine does not change in 300 gL^{-1} 70 kDa Ficoll or its monomer, sucrose.[18,22] Information about crowding induced changes in intrinsic rates can also be gleaned from unstructured loops of globular proteins.

Chymotrypsin inhibitor 2 [CI2; Fig. 1(A)] is a globular protein[25] [Fig. 1(A)] that has been extensively studied by amide $^{1}H/^{2}H$ exchange.[13,19,26,27] Residues in its reactive loop are potential models for assessing k_{int}, because they possess few hydrogen bonds, lower than average order parameters,[28] high B-factors,[25] and large solvent accessible surface areas [SASAs; Fig. 1(B)]. Phase-modulated CLEAN chemical exchange (CLEANEX-PM) experiments[29] conducted in buffer and under crowded conditions show that exchange rates in the loop do not change in solutions containing 300 gL^{-1} 40-kDa poly-vinylpyrrolidone (PVP),[19] 100 gL^{-1} lysozyme, and 100 gL^{-1} bovine serum albumin.[20] These observations suggest that k_{int} values in buffer can be applied to experiments conducted with these crowding agents.

To understand protein stability under native cellular conditions, we must understand how the cytoplasm affects k_{int}. This goal is challenging because ^{15}N-^{1}H heteronuclear single quantum correlation spectra cannot be observed from most globular proteins, including CI2, in *E. coli* cells.[30–32] Furthermore, proteins often begin to leak from cells after 1.5 h,[33] or less, whereas the experiments used to measure exchange require at least an order of magnitude longer.[29,34] For these reasons, we chose *E. coli* cell lysates as a reasonable mimic of the cytoplasm.

We used a modified $^{15}N^{H/D}$-SOLEXSY[34] experiment to measure k_{int}. The experiment is performed on a $^{15}N/^{13}C$ doubly labeled protein, in 50% $^{1}H_{2}0$:50% $^{2}H_{2}O$. SOLEXSY bypasses problems such as radiation damping artifacts, long recycle delays, nuclear Overhauser effect-type and total correlation spectroscopy-type transfers between $^{1}H^{\alpha}$ and $^{1}H^{N}$, and relayed transfer that arise from selective water excitation.[34] Instead, magnetization is transferred from the $^{1}H^{\alpha}$ through the $^{13}C^{\alpha}$ and carbonyl carbon to the amide ^{15}N. The ^{15}N chemical shift is then encoded to produce two signals, $^{15}N^{D}$ and $^{15}N^{H}$.

After encoding, a variable mixing time monitors the exchange of $^{15}N^{D}$ and $^{15}N^{H}$ for each hydrogen isotope, and magnetization is transferred back to ^{1}H for detection. At short mixing times, only protonated species are observed, because only protonated amide nitrogens are detected at the ^{1}H frequency (Fig. 2). The chemical shift of $^{15}N^{D}$ is also recorded, but at short mixing times no signal is detected because little ^{1}H has exchanged onto the deuterated amide. At longer times, exchange of ^{1}H onto the initially deuterated ($^{15}N^{D}$) site causes an increase in the volume of the $^{15}N^{D}/^{1}H$ cross-peak, producing a buildup curve [Fig. 2(B)]. The exchange of deuterons onto the initially protonated site causes a decrease in volume, and a corresponding decay with time [Fig. 2(B)]. Plots of peak volume versus time can be fitted to yield k_{int}. High-quality data can be obtained for rates between 0.3 and 5.0 s^{-1}.[34]

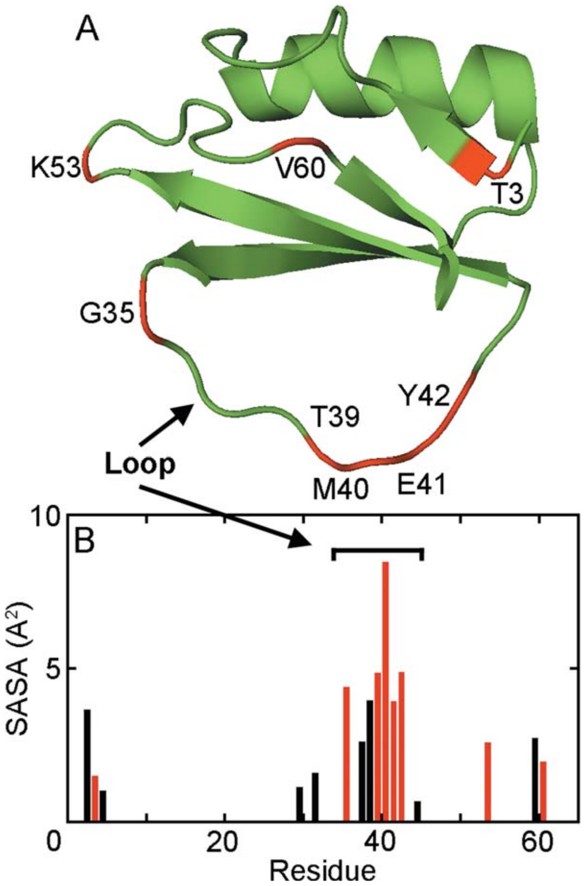

Figure 1. Exposed and fast exchanging backbone amide protons in CI2. Residues whose backbone amide protons exhibit reliable exchange using SOLEXSY (293 K, 50 m*M* sodium phosphate, pH_{read} 6.7) are shown in red. (A) Ribbon diagram (PDB: 2CI2 made with PyMOL[23]). (B) Histogram of SASAs of backbone amide nitrogens versus residue number. Residues whose backbone amide hydrogens form a hydrogen bond to a backbone carbonyl oxygen, a side chain oxygen or the oxygen of structured water are not shown, with one exception (see text). SASAs were calculated with the program POPS.[24]

We crowded CI2 with up to 100 g dry weight L^{-1} ($g_{dry}L^{-1}$) of *E. coli* lysate and used $^{15}N^{H/D}$-SOLEXSY[34] to measure exchange in the dynamic loop and other exposed regions. Exchange rates are

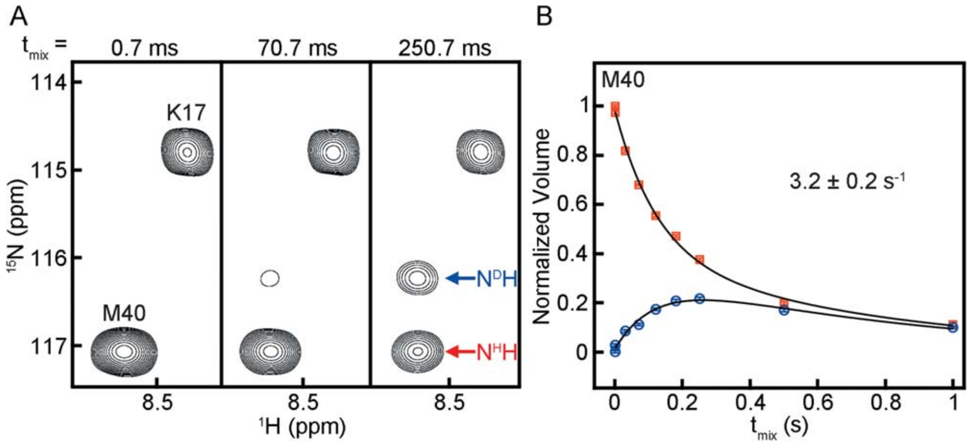

Figure 2. Region of $^{15}N^{H/D}$-^{1}H correlation spectra (A) showing an exchangeable (M40) and a nonexchangeable (K17) residue from CI2 and (B) the corresponding exchange curves for M40. Buildup of the deuterated amide ($N^{D}H$) and decay of the protonated amide ($N^{H}H$) occur as the mixing time (t_{mix}) increases. Spectra were acquired with a modified SOLEXSY pulse sequence (see Materials and Methods section).

largely unchanged in lysates compared to buffer alone. Our results suggest that k_{int} values from buffer-based experiments (i.e., from SPHERE) are valid for quantifying protein stability under cellular conditions.

Results

Lysate solutions are problematic for two reasons. First, at high concentrations they are not stable enough to allow acquisition of a full 60-h SOLEXSY experiment (Fig. 3). Second, weak interactions between constituents of the lysate and the protein being studied result in a shorter transverse relaxation time (T_2), leading to broad resonances that degrade the quality of the spectra used to create buildup and decay curves.[35–37]

In an attempt to overcome the stability problem, we decreased the acquisition time by reducing the number of scans, but this approach exacerbated the broadening problem. We then tried removing the sign-coding portion of the SOLEXSY experiment. In combination with acquiring fewer t_1 points, this change enabled us to acquire a complete experiment in 15 h. Furthermore, the consequent removal of 10.6 ms ($\sim\frac{1}{J_{NH}}$) from the pulse sequence resulted in a mean increase in signal to noise ratio of 25% in buffer [depending on the resonance, Supporting Information Fig. S1(A)], which helped compensate for the decreased sensitivity arising from the shorter T_2 values in lysate [Supporting Information Fig. S1(B)]. The original and modified SOLEXSY experiments were validated by comparing rates acquired in buffer to mathematical predictions and to values obtained with CLEANEX-PM[9,20] (Supporting Information Table S1).

Residues useful for assessing k_{int} values should lack stable hydrogen bonds. Backbone amide hydrogens from 15 residues of CI2 do not form hydrogen bonds to a backbone carbonyl oxygen, a side chain oxygen, or the oxygen of structured water.[25] These residues are in loops, and as expected, exhibit significant SASAs [Fig. 1(B)]. We also included E41, whose backbone amide ^{1}H is within hydrogen bonding distance (2.6 Å for the heavy atoms) of the carbonyl oxygen of T39, in our analysis because loop motion likely makes any hydrogen bond transient.

Nine of these 16 hydrogens exhibit amide exchange on the SOLEXSY (i.e., 0.3–5.0 s^{-1})[34] timescale [Fig. 4(A); Supporting Information Table S1 and Figs. S2 and S3]. Data from K2, were not included because its exchange is faster than that which can be reliably measured by SOLEXSY.[34] Values obtained in buffer and in 100 $g_{dry}L^{-1}$ lysate are within error of one another, and are similar to the values calculated and predicted by SPHERE [Fig. 4(A), Supporting Information Table S1].

Seven of the 16 residues do not show exchange on the SOLEXSY time scale at pH_{corr} 6.9 (Fig. 1). Residues E4 and Q59 exchange slow enough to be detected by conventional $^{1}H_2O$-to-$^{2}H_2O$ transfer experiments.[13,18] The other five residues (A29, V31, H37, V38, I44) show chemical exchange using CLEANEX-PM, but these data were acquired at higher pH.[9] Extrapolating these data to our conditions (pOH = 7.71)[38] and using an Arrhenius activation energy (E_a)[14] of 17 kcalmol^{-1}, leads to k_{int} values between 0.001 and 0.04 s^{-1}, which are too small to be accurately assessed with SOLEXSY.

Discussion

Knowing how the cytoplasm affects $^{1}H/^{2}H$ amide exchange of exposed residues is vital to calculating opening free energies and global stabilities.[10,18,19] Although these values are normally obtained from SPHERE, the server only predicts values in solutions made with 100% $^{1}H_2O$ or $^{2}H_2O$. The SOLEXSY

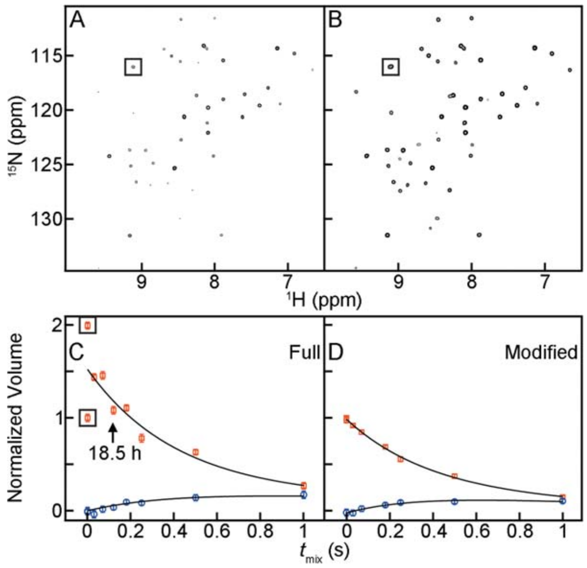

Figure 3. Reconstituted lysate (100 $g_{dry}L^{-1}$) is stable for 15 h, but is compromised in less than 59 h. t_{mix} values were acquired in random order. The SOLEXSY dataset for the shortest t_{mix}, 0.7 ms, was acquired twice; the second time at the end of the experiment. The full SOLEXSY experiment required ~59 h, whereas the modified experiment required <15 h. (A) Spectrum recorded with the full SOLEXSY experiment (t_{mix} = 0.7 ms) at 6 h. The G35 cross-peak is boxed. (B) Repeat spectrum (i.e., t_{mix} = 0.7 ms) recorded to assess stability at the end of the experiment, 59 h, 16 m. Peak volumes are larger at the end of the experiment. The increased volume suggests precipitation of the lysate, allowing CI2 more rotational freedom, lengthening T_2, which sharpens the resonances. (C) Fit for G35 from the full SOLEXSY experiment, which required 59 h. Instead of decaying, the volume of the 120-ms point (vertical arrow, acquired at ~19 h) is greater than that for the 0.7-ms point, acquired at 6 h, indicating breakdown of the lysate. Consistent with this idea, precipitate was visible at ~60 h. (D) G35 data acquired with the modified experiment, which required only ~15 h. The repeated t_{mix} point, acquired at 14 h, is on top of the point acquired at 1 h, suggesting that the lysate was stable over the course of the modified experiment. Consistent with this idea, no precipitate was observed at the end of the experiment.

experiment, however, is conducted in a 1:1 $^{2}H_2O$:$^{1}H_2O$ mixture. To obtain a direct comparison to our solution conditions, we calculated the rates using the equations that drive SPHERE, but with different parameters. Rates were calculated stipulating a buffer made from 1:1 $^{2}H_2O$:$^{1}H_2O$ (pH_{corr} 6.9, pK_W 14.61), with poly-DL-alanine as the reference molecule and $k_{b,ref}$ for N^D exchanging in $^{1}H_2O$.[14–16,38] These rates were then halved[34] to make them comparable to those from experiment and SPHERE. This manipulation accounts for the fact that exchange onto $^{15}N^D$ is only visible by SOLEXSY when ^{1}H exchanges. In other words, ^{2}H exchange onto initially deuterated amides is undetected, because only ^{1}H is visible at the ^{1}H frequency, making the predicted rate twice that measured by SOLEXSY. These corrected values closely match those obtained from SPHERE by using the poly-DL-alanine rate basis, with a pH_{read} 6.5, in 100% $^{2}H_2O$ (Supporting Information Table S1).

The corrected rates are also similar to rates measured in buffer [Fig. 4(A)] and obtained with CLEANEX-PM (Supporting Information Table S1).[9,20] Slight deviations from the CLEANEX-PM results are likely due to differences in solvent condition; the SOLEXSY experiments used 1:1 $^{2}H_2O$:$^{1}H_2O$ and a different ionic strength. Taken together, these results suggest that SOLEXSY is a useful experiment for measuring exchange rates in disordered loops of globular proteins.

The rates are also similar to those measured in lysate (Fig. 4), indicating that lysate at 100 $g_{dry}L^{-1}$ has an insignificant effect on exchange. Protection factors (k_{int}/k_{obs}) of less than five are an unreliable indicator of secondary structure,[39] whereas residues that exchange only on complete unfolding (i.e., globally exchanging residues) can have protection factors greater than 10^5.[13,18,19,27,40] Protection factors based on the SOLEXSY data ($k_{int,predicted}/k_{obs,buffer}$ and $k_{int,predicted}/k_{obs,lysate}$), are no larger than five for the loop region (Fig. 4), and even these may reflect small errors in the parameters used to drive SPHERE.

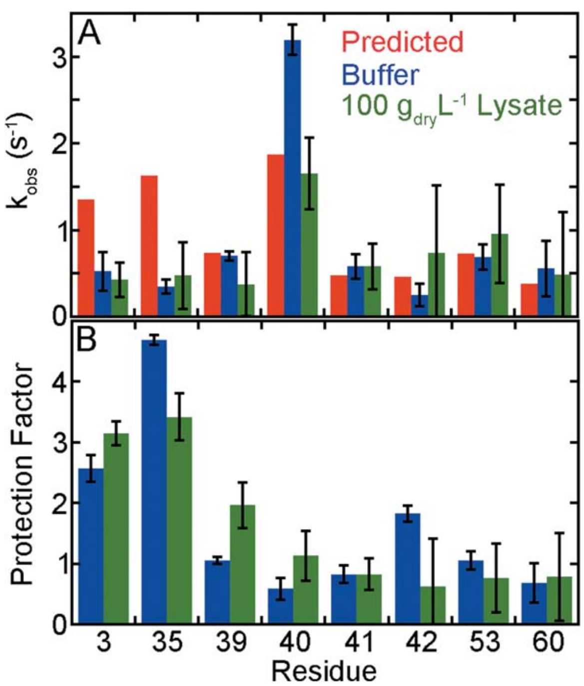

Figure 4. *E. coli* lysate (100 $g_{dry}L^{-1}$, green) and buffer alone (blue) yield similar amide backbone ^{1}H exchange rate constants, k_{obs}, for solvent accessible residues. (A) Predicted values[14,15] are shown in red. Values from modified SOLEXSY data are the average of 20 Monte Carlo noise simulations. Error bars represent the standard deviation of the mean. (B) Protection factors ($k_{int,predicted}/k_{obs,buffer}$ and $k_{int,predicted}/k_{obs,lysate}$). Error bars are from the uncertainties in Panel A. Conditions are given in the caption of Figure 1.

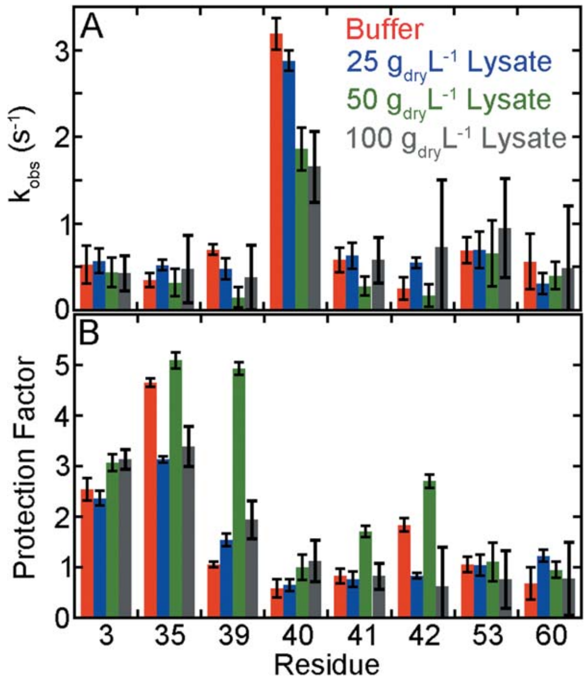

Figure 5. Comparison of 0–100 $g_{dry}L^{-1}$ lysate show no general and consistent trend. (A) Values from SOLEXSY data are the average of 20 Monte Carlo noise simulations. Error bars represent the standard deviation of the mean. Data were acquired with the modified SOLEXSY experiment for buffer and 100 $g_{dry}L^{-1}$ lysate. The full experiment was used for 25 and 50 $g_{dry}L^{-1}$ lysate. (B) Protection factors ($k_{int,predicted}/k_{obs,SOLEXSY}$). Predicted values were calculated as described in the footnote to Supporting Information Table S1. Error bars are the same as in Panel A. Protection factors of less than five are not a reliable predictor of structure.[39]

Taken together, the data indicate that small differences in k_{obs} values between lysate and buffer will have small effects on protein stability studies conducted in lysates.

The concentration of macromolecules in the cytoplasm of *E. coli* is 300 gL^{-1}, or even higher.[1,2] Our attempts to acquire SOLEXSY data at these concentrations were unsuccessful for the reasons discussed above: chemical instability of the lysate and interaction-induced resonance broadening. Nevertheless, rates obtained in 0, 25, 50, and 100 $g_{dry}L^{-1}$ lysate show no general and consistent trend (Fig. 5 and Supporting Information Fig. S4), suggesting our results are applicable to the dense interior of the bacterial cell.

Materials and Methods

Protein

^{13}C glucose (2.0 gL^{-1}) and $^{15}NH_4Cl$ (1.0 gL^{-1}) were used to produce purified CI2.[19,37]

Lysate

Lysates were obtained by modifying the method described by Wang *et al.*[37] Competent BL21-DE3 (Gold) *E. coli* were transformed with the pET28a vector harboring the kanamycin resistance gene. The transformants were plated on Luria-Bertani (LB) agar plates containing 60 μg/mL kanamycin. The plates were incubated overnight at 37°C. A single colony was added to 60 mL of LB liquid media containing 60 μg/mL kanamycin. The culture was shaken overnight (New Brunswick Scientific, Innova, I26) at 225 rpm and 37°C, then equally divided into four, 2.8-L baffled flasks, each containing 1 L of LB and 60 μg/mL kanamycin. This culture was grown to saturation (9 h). The cells were pelleted at 6500*g* for 30 min and the pellets stored at −20°C.

Each frozen cell pellet was thawed, resuspended and lysed in 25 mL of 25 m*M* tris (pH 7.6) containing a cocktail of protease inhibitors [Sigma-Aldrich: 0.02 m*M* 4-(2-aminoethyl) benzenesulfonyl fluoride, 0.14μ*M* E-64, 1.30 μ*M* bestatin, 0.01 μ*M* leupeptin, 3.0 n*M* aprotinin and 0.01 m*M* sodium EDTA, and 0.01 m*M* final concentrations]. Lysis was accomplished by sonic dismembration on ice for 6 min (Fischer Scientific, Sonic Dismembrator Model 500, 20% amplitude, 2 s on, 2 s off). After lysis, cell debris was removed by centrifugation (14,000*g* at 10°C for 40 min). The supernatant was filtered through a 0.22 μm Durapore® PVDF membrane (Millipore).

The filtrates were pooled and dialyzed (Thermo Scientific, SnakeSkin, 3K MWCO) at 4°C against 5 L of 10 m*M* tris, 0.1% NaN_3 (pH 7.6) for 72 h. The buffer was changed every 24 h. The inhibitor cocktail was added to each dialysate. After lyophilization (Labconco, Freezone Plus 2.5), the straw-colored powder was stored at -20°C. To ensure that the lysate contained 50% exchangeable protons and 50% exchangeable deuterons, the powder was resuspended in 50% D_2O (Cambridge Isotopes Laboratories), incubated at room temperature for 8 h and lyophilized. The process was performed twice and the resultant powder (300.0 mg) was resuspended in sufficient 50% deuterated sodium phosphate buffer (50 m*M*, pH_{read} 6.7) to give 3.0 mL of solution with a final concentration of 1.0×10^2 g dry weight L^{-1}. The pH_{read} was adjusted to 6.7. The solution was centrifuged at 14000 *g* for 10 min. The supernatant contained 52 ± 4 gL^{-1} of protein as determined by a modified Lowry assay (Thermo Scientific). The uncertainty in the concentration is the standard deviation of the mean from triplicate measurements.

Nuclear magnetic resonance

^{13}C, ^{15}N-enriched CI2 was added to sodium phosphate buffer (50 m*M*, 50% ^1H_2O:50% ^2H_2O, pH_{read} 6.7) with and without lysate. The final CI2 concentration was ∼1 m*M* for samples acquired in buffer alone with the modified SOLEXSY experiment. A concentration of 1.5 m*M* was used for all other experiments. The concentrations in buffer were verified by measuring the absorbance at 280.0 nm ($\varepsilon = 7.04 \times 10^3 M^{-1}$ cm $^{-1}$).[41]

A modified SOLEXSY experiment[34] was used to measure exchange rates. Sign coding was originally used to facilitate data acquition on intrinsically disordered proteins by reducing the number of cross-peaks.[34] The spectra of globular proteins like CI2 are well dispersed, elimiating the need for this feature. We removed the 10.6-ms sign-coding period, $\left(\frac{1}{2J_{\mathrm{NH}}}\right) - 90^\circ_x 90^\circ_{\pm x}(^1\mathrm{H}), ^{180^\circ_x(^{15}\mathrm{N}) - \left(\frac{1}{2J_{\mathrm{NH}}}\right)}$. Data were acquired at 293 K on a 600-MHz Bruker Avance III HD spectrometer equipped with a HCN triple resonance cryoprobe (Bruker TCI) and Topspin Version 3.2 software. Sweep widths were 9600 Hz in the ^{1}H dimension and 2300 Hz in the ^{15}N dimension. Twenty-four transients were collected using 1024 complex points in t_2 with 128 TPPI points in t_1 for each mixing time. Data were collected in a pseudo-3D mode with mixing times of 0.7, 1000.7, 250.7, 120.7, 30.7, 180.7, 70.7, and 500.7 ms. An additional spectrum with a 0.7-ms mixing time was collected at the end of the experiment to assess lysate stability. The 120.7-ms data point was omitted for the 100 $\mathrm{g_{dry}L^{-1}}$ lysate. Acquisition required ~15 h per sample. The full experiment used the same parameters, except that 256 points in t_1 were used for each mixing time, and required ~60 h per sample.

Data processing

Data were processed with NMRPipe.[42] The t_2 data were subjected to a 60° shifted squared sine bell function (800 complex points for buffer alone and 512 complex points for lysate) before zero-filling to 8096 points and Fourier transfomation. The t_1 data were linear predicted to 256 points before application of a 60°-shifted squared sine bell. The t_1 data were then zero-filled to 2048 points and Fourier-transformed. The spectra were peak picked and integrated using the built in automated routines. Peak volumes were fitted as described.[34] When the full experiment was used similar routines were followed without linear prediction. Sign encoded spectra were added or subtracted to create buildup and decay spectra, respectively.

Acknowledgments

The authors thank Nikolai Skrynnikov and Veniamin Chevelkov for providing SOLEXSY codes and assisting with their application and Elizabeth Pielak for insightful comments on the manuscript.

References

1. McGuffee SR, Elcock AH (2010) Diffusion, crowding & protein stability in a dynamic molecular model of the bacterial cytoplasm. PLoS Comput Biol 6:e1000694.
2. Zimmerman SB, Trach SO (1991) Estimation of macromolecule concentrations and excluded volume effects for the cytoplasm of *Escherichia coli*. J Mol Biol 222:599–620.
3. Zhou HX, Rivas G, Minton AP (2008) Macromolecular crowding and confinement: biochemical, biophysical, and potential physiological consequences. Annu Rev Biophys 37:375–397.
4. Elcock AH (2010) Models of macromolecular crowding effects and the need for quantitative comparisons with experiment. Curr Opin Struct Biol 20:196–206.
5. Hvidt A, Linderstrøm-Lang K (1954) Exchange of hydrogen atoms in insulin with deuterium atoms in aqueous solutions. Biochim Biophys Acta 14:574–575.
6. Berger A, Linderstrøm-Lang K (1957) Deuterium exchange of poly-DL-alanine in aqueous solution. Arch Biochem Biophys 69:106–118.
7. Englander SW, Mayne L, Bai Y, Sosnick TR (1997) Hydrogen exchange: the modern legacy of Linderstrøm-Lang. Protein Sci 6:1101–1109.
8. Englander SW, Kallenbach NR (1983) Hydrogen exchange and structural dynamics of proteins and nucleic acids. Q Rev Biophys 16:521–655.
9. Hernández G, Anderson JS, LeMaster DM (2009) Polarization and polarizability assessed by protein amide acidity. Biochemistry 48:6482–6494.
10. Miklos AC, Li C, Pielak GJ (2009) Using NMR-detected backbone amide ^{1}H exchange to assess macromolecular crowding effects on globular-protein stability. Methods Enzymol 466:1–18.
11. Hvidt A, Nielsen SO (1966) Hydrogen exchange in proteins. Adv Protein Chem 21:287–386.
12. Bai Y, Milne JS, Mayne L, Englander SW (1994) Protein stability parameters measured by hydrogen exchange. Proteins 20:4–14.
13. Neira JL, Itzhaki LS, Otzen DE, Davis B, Fersht AR (1997) Hydrogen exchange in chymotrypsin inhibitor 2 probed by mutagenesis. J Mol Biol 270:99–110.
14. Bai Y, Milne JS, Mayne L, Englander SW (1993) Primary structure effects on peptide group hydrogen exchange. Proteins 17:75–86.
15. Connelly GP, Bai Y, Jeng MF, Englander SW (1993) Isotope effects in peptide group hydrogen exchange. Proteins 17:87–92.
16. Molday RS, Englander SW, Kallen RG (1972) Primary structure effects on peptide group hydrogen exchange. Biochemistry 11:150–158.
17. Zhang Y-Z (1995) Protein and peptide structure and interactions studied by hydrogen exchange and NMR. Ph.D. Dissertation, University of Pennsylvania, Philadelphia.
18. Benton LA, Smith AE, Young GB, Pielak GJ (2012) Unexpected effects of macromolecular crowding on protein stability. Biochemistry 51:9773–9775.
19. Charlton LM, Barnes CO, Li C, Orans J, Young GB, Pielak GJ (2008) Residue-level interrogation of macromolecular crowding effects on protein stability. J Am Chem Soc 130:6826–6830.
20. Miklos AC, Sarkar M, Wang Y, Pielak GJ (2011) Protein crowding tunes protein stability. J Am Chem Soc 133:7116–7120.
21. Wang Y, Sarkar M, Smith AE, Krois AS, Pielak GJ (2012) Macromolecular crowding and protein stability. J Am Chem Soc 134:16614–16618.
22. Wang A, Robertson AD, Bolen DW (1995) Effects of a naturally occurring compatible osmolyte on the internal dynamics of ribonuclease A. Biochemistry 34: 15096–15104.

23. The PyMOL Molecular Graphics System, Version 1.3. Schrödinger, LLC. Available at: www.pymol.org. Last accessed: 2010.
24. Cavallo L, Kleinjung J, Fraternali F (2003) POPS: a fast algorithm for solvent accessible surface areas at atomic and residue level. Nucleic Acids Res 31:3364–3366.
25. McPhalen CA, James MN (1987) Crystal and molecular structure of the serine proteinase inhibitor CI-2 from barley seeds. Biochemistry 26:261–269.
26. De Prat Gay G, Ruiz-Sanz J, Neira JL, Itzhaki LS, Fersht AR (1995) Folding of a nascent polypeptide chain in vitro: cooperative formation of structure in a protein module. Proc Natl Acad Sci U S A 92:3683–3686.
27. Itzhaki LS, Neira JL, Fersht AR (1997) Hydrogen exchange in chymotrypsin inhibitor 2 probed by denaturants and temperature. J Mol Biol 270:89–98.
28. Shaw GL, Davis B, Keeler J, Fersht AR (1995) Backbone dynamics of chymotrypsin inhibitor 2: effect of breaking the active site bond and its implications for the mechanism of inhibition of serine proteases. Biochemistry 34:2225–2233.
29. Hwang TL, van Zijl PC, Mori S (1998) Accurate quantitation of water-amide proton exchange rates using the phase-modulated CLEAN chemical exchange (CLEANEX-PM) approach with a fast-HSQC (FHSQC) detection scheme. J Biomol NMR 11:221–226.
30. Li C, Charlton LM, Lakkavaram A, Seagle C, Wang G, Young GB, Macdonald JM, Pielak GJ (2008) Differential dynamical effects of macromolecular crowding on an intrinsically disordered protein and a globular protein: implications for in-cell NMR spectroscopy. J Am Chem Soc 130:6310–6311.
31. Li C, Wang G-F, Wang Y, Creager-Allen R, Lutz EA, Scronce H, Slade KM, Ruf RAS, Mehl RA, Pielak GJ (2009) Protein ^{19}F NMR in Escherichia coli. J Am Chem Soc 132:321–327.
32. Barnes CO, Monteith WB, Pielak GJ (2011) Internal and global protein motion assessed with a fusion construct and in-cell NMR spectroscopy. ChemBioChem 12:390–391.
33. Barnes CO, Pielak GJ (2011) In-cell protein NMR and protein leakage. Proteins 79:347–351.
34. Chevelkov V, Xue Y, Rao DK, Forman-Kay JD, Skrynnikov NR (2010) ^{15}N H/D-SOLEXSY experiment for accurate measurement of amide solvent exchange rates: application to denatured drkN SH3. J Biomol NMR 46:227–244.
35. Li C, Pielak GJ (2009) Using NMR to distinguish viscosity effects from nonspecific protein binding under crowded conditions J Am Chem Soc 131:1368–1369.
36. Li C, Wang Y, Pielak GJ (2009) Translational and rotational diffusion of a small globular protein under crowded conditions. J Phys Chem B 113:13390–13392.
37. Wang Y, Li C, Pielak GJ (2010) Effects of proteins on protein diffusion. J Am Chem Soc 132:9392–9397.
38. Covington AK, Robinson RA, Bates RG (1966) The ionization constant of deuterium oxide from 5 to 50°. J Phys Chem 70:3820–3824.
39. Mori S, van Zijl PCM, Shortle D (1997) Measurement of water–amide proton exchange rates in the denatured state of staphylococcal nuclease by a magnetization transfer technique. Proteins 28:325–332.
40. Miklos AC, Li C, Sharaf NG, Pielak GJ (2010) Volume exclusion and soft interaction effects on protein stability under crowded conditions. Biochemistry 49:6984–6991.
41. Roesler KR, Rao AG (1999) Conformation and stability of barley chymotrypsin inhibitor-2 (CI-2) mutants containing multiple lysine substitutions. Protein Eng 12: 967–973.
42. Delaglio F, Grzesiek S, Vuister GW, Zhu G, Pfeifer J, Bax A (1995) NMRPipe: a multidimensional spectral processing system based on UNIX pipes. J Biomol NMR 6:277–293.